Modelling the Stratigraphy and Geoarchaeology of English Valley Systems

Quintijn Clevis, Gregory E. Tucker, Gary Lock, Arnaud Desitter

Project 3299

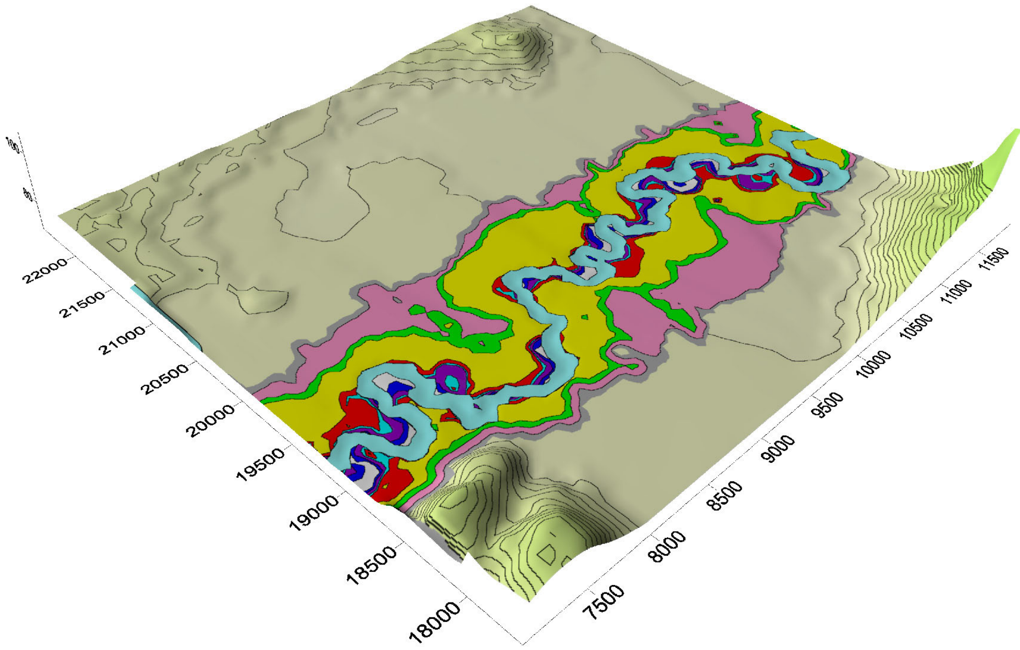

March 2004

English Heritage

Modelling the Stratigraphy and Geoarchaeology of English Valley Systems

Quintijn Clevis, Gregory Tucker, Gary Lock, Arnaud Desitter
School of Geography and the Environment
Oxford University

Project number 3299

http://www.geog.ox.ac.uk/research/projects/evs/

1. Summary

This report summarises the activities and accomplishments related to the project during the period April 2003 through February 2004. The main achievements during this period were:

- Construction of an ArcInfo GIS containing photo-archaeological data on the Upper Thames Valley.
- Modification and debugging of the CHILD software in order to make it suitable for geoarchaeological simulations of lowland meander-floodplain systems.
- Write auxiliary visualisation software for displaying animations of floodplain evolution and the three-dimensional structure of the subsurface stratigraphy.
- Conduct two sets of model experiments exploring the sensitivity of the model to key variables and scenarios of Holocene climate change.

For the Holocene scenarios we followed a recent paper by Lewin and Macklin (2003) in which frequency by age analyses of terraces and paleo-meander bends across the United Kingdom was used to conclude that the preservation of alluvial units increased throughout the Holocene. They found a skewed frequency distribution with a higher number of younger units since the Neolithic and interpreted this pattern as the effect of increased sediment flux to fluvial systems by anthropogenic land-use. In addition, they argue that pronounced presence of some alluvial units, diverging from this general trend, correspond to short-lived Central European cold-humid phases (Haas *et al.*, 1998).

Model results confirm that the preservation potential of alluvial units is high in generally aggrading systems and that less than 20% of the stratigraphy is lost by the

reworking effect of meandering. However, the spatio-temporal complexities of the river meandering process make it difficult to correlate centennial climatic perturbations of the type recognised by Haas *et al.* (1998) to the preservation characteristics of the stratigraphy. The system's response to perturbations in storm intensity or increases in overbank sedimentation rate is associated with time lags, which are normally longer than the time-scale of the climatic perturbation. Intensification of the mean storm rainfall rate for example decreases the volume and preservation potential of fluvial units deposited 500-1500 yrs after this perturbation. In addition, the effects of multiple perturbations interfere with each other and make discrimination of individual climate perturbations ambiguous. If this behaviour is to be expected for real systems it would make deduction of climatic variation based on simple tools such as fluvial unit – frequency plots almost impossible without independent evidence for climatic change.

2. GIS database & data compilation

We have compiled an archaeological geographic information system (GIS) on the Upper Thames Valley using standard ArcInfo software. Basic data layers in the GIS include a digital terrain model of the Upper Thames Valley with a resolution of 50 meter (Figure 1) and information from Ordinance Survey maps. The digital terrain data in the GIS were used as surface boundary condition in the model simulations presented below. These simulations include a small study of historical hillslope erosion in the Uffington White Horse area (Figure 2) and a more extensive investigation of Holocene floodplain evolution linked to subsurface stratigraphy.

The base data layers in the GIS are combined with an aerial photographic dataset on crop marks and archaeological landscape features, obtained from the NMR offices in Swindon. These photo-archaeological data are originally gathered and interpreted as part of the Thames Valley Mapping Project (Fenner and Dyer, 1994), but until now they were never combined within a modern ArcInfo GIS system. Two snapshots of the GIS are shown in figure 3, illustrating the density of crop marks within the floodplain of the Thames and on the more protected gravel terraces, further away from the river. The archaeological GIS could be made available on CD or the Internet via the project website but this requires permission of the NMR.

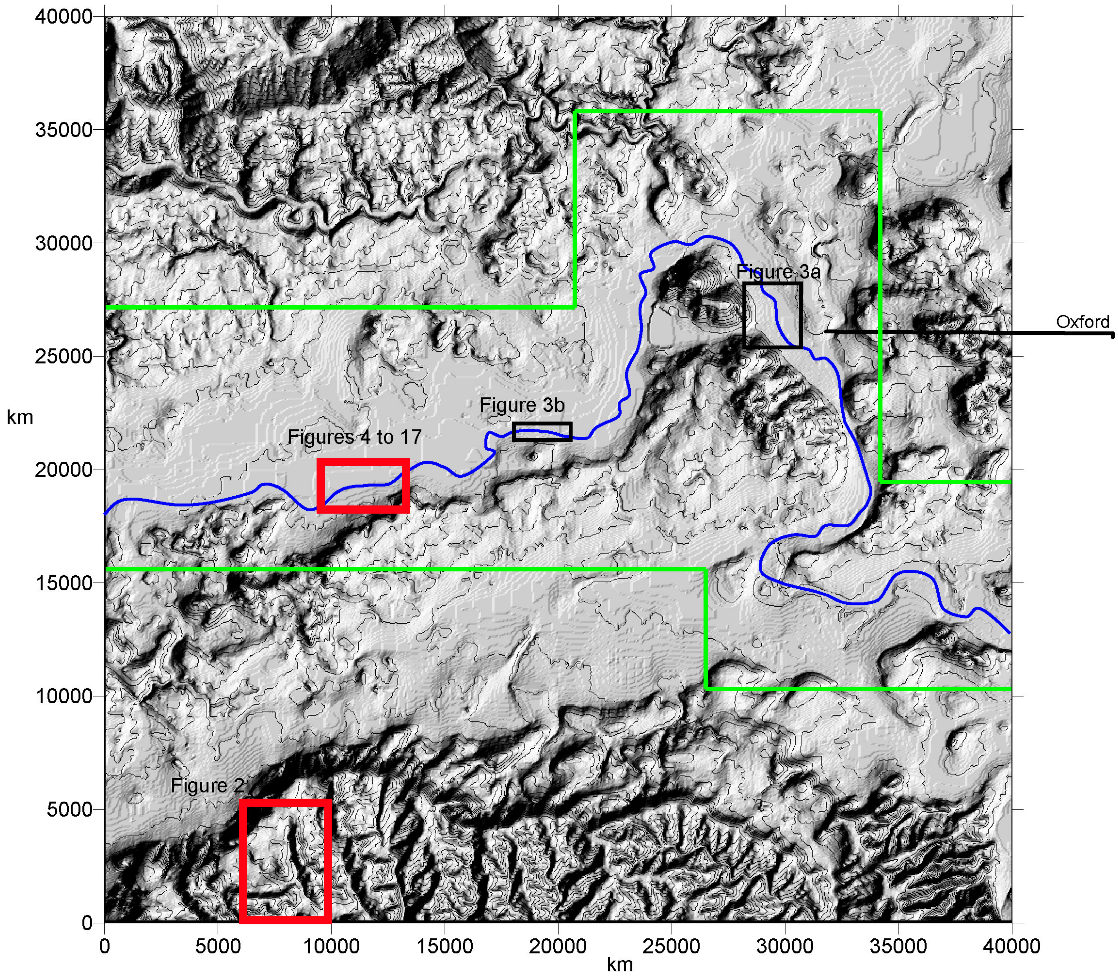

Figure 1. Overview of the Upper Thames Valley, west of Oxford. Indicated are the extension of the aerial photo-archaeological GIS (green), and the location of the two study areas (red) used in the modelling study.

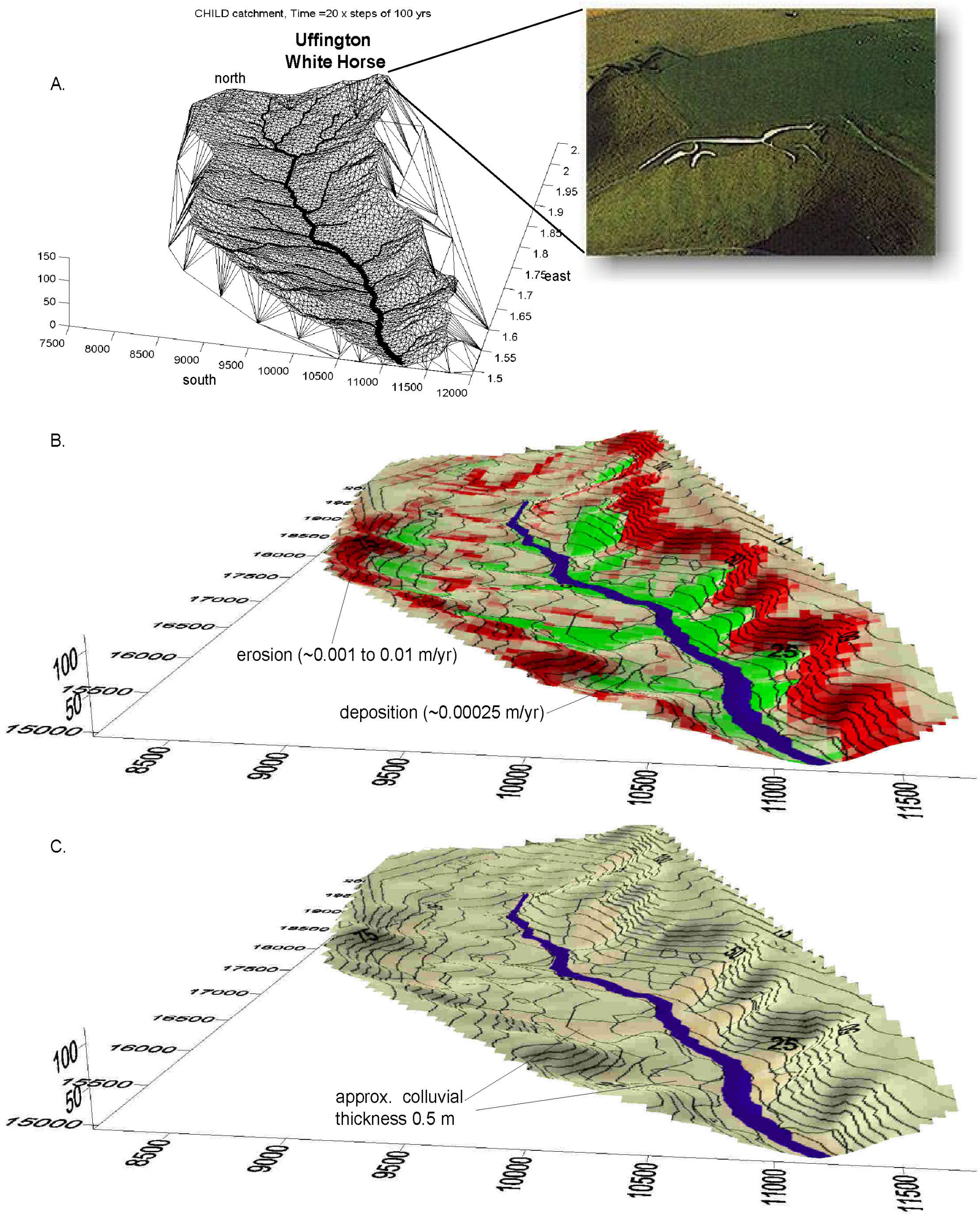

Figure 2. Examples of simulation of land clearance-induced erosion in the Weathercock/ Maddle Farm valley in the Berkshire downs. A) Computational mesh used by the model B) Erosion and depostion pattern, note that most of the eroded material is transported out of the modelled valley towards downstream floodplains.
C) Accummulated alluvium in the valley after 2000 yrs of erosion.

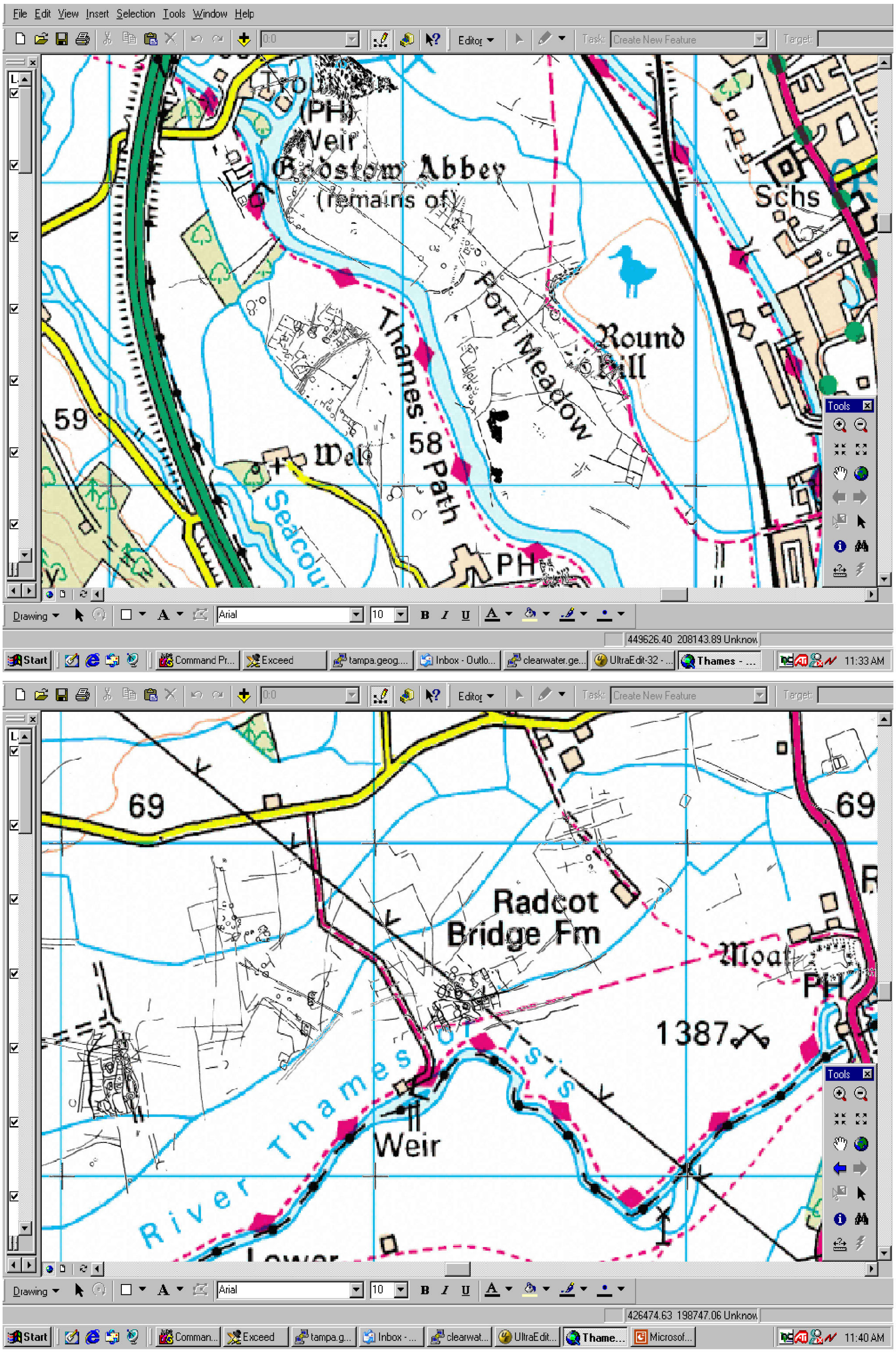

Figure 3. Snapshots of the archaeological GIS constructed during this study. A) Crop marks (thin black lines) in the floodplain of the Thames river immediately west of Oxford. B) Crop marks located on the gravel terraces near Radcot Bridge, approximately 6 miles west of Oxford.

3. Methodology

Simulation of channel migration and meandering

All simulations in this study were performed used the CHILD model. CHILD is a distributed model of landscape erosion, sediment deposition, topographic evolution and stratigraphy accummulation (Figure 4). Many of the software modifications and improvements made to the model during this project were aimed at making CHILD suitable for geo-archaeological and stratigraphic simulations.

In CHILD the landscape is represented by an irregular network of nodes, which is updated every simulation timestep using Delauney triangulation. This dynamic remeshing capability makes it suited for modelling complex forms such as meander bends and their gradual development over time. During the meandering process obstructing nodes are deleted while additional nodes are created to form point bars. The main principle applied in the meander model is called 'topographic steering' (Dietrich & Smith, 1983; Smith & McLean, 1984), which is based on the observation that secondary flows over the bed topography translate the eroding high-velocity flow in a channel laterally. This results in transfer of momentum and maximum shear stress towards the outer bank and downstream (Figure 5). The rate at which channel nodes are allowed to migrate is defined by the rate of bank erosion, which is proportional to this bank shear stress.

$$R_{migration} = E\tau\hat{n} \qquad (1)$$

where E is the bank erodability coefficient, the bank shear stress and n the unit vector perpendicular to the downstream direction. The bank shear stress in a point '*s'* along the meandering channel is found by summing contributions of lateral force increments dF_n generated by upstream nodes '*s' '* according to a Gaussian function.

$$\tau_w(s) = \frac{\sum_{s'} \exp\left[\frac{-\left\{s-\left[s'+L(s')\right]\right\}^2}{2\lambda^2}\right] dF_n(s')}{\sqrt{2\pi\lambda H}} \qquad (2)$$

where H represents the average flow depth. L the distance between an upstream segment s' and the zone of maximum bank shear stress affected by its lateral force increment (e.g outer cut bank), and and the shear stress-dissipation length scale.

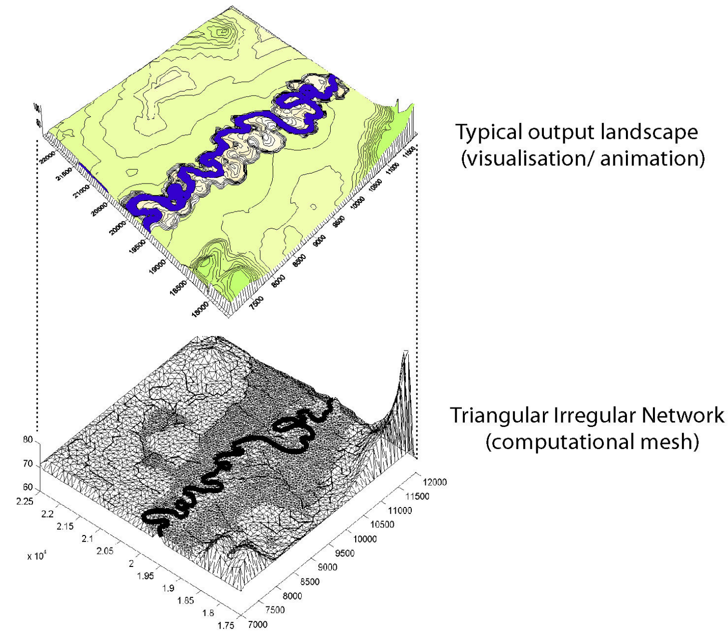

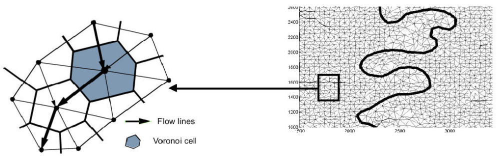

Figure 4a. Illustration of the triangular framework used for the computation of erosion, deposition and meandering in the CHILD model. Indicated in the box are the steepest descent flow routing over the nodes and the Voronoi areas represented by the nodes.

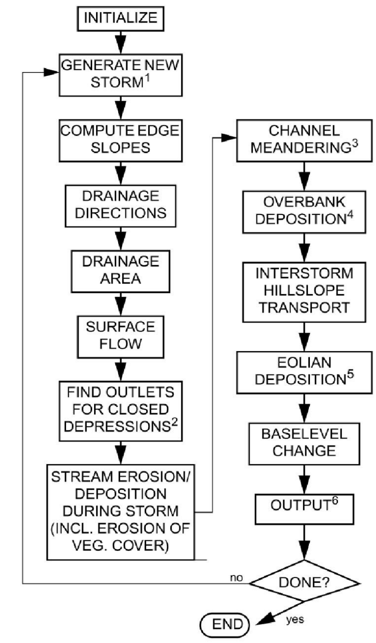

Figure 4b. Simplified flow chart of the geomorphic procedures in the CHILD model.

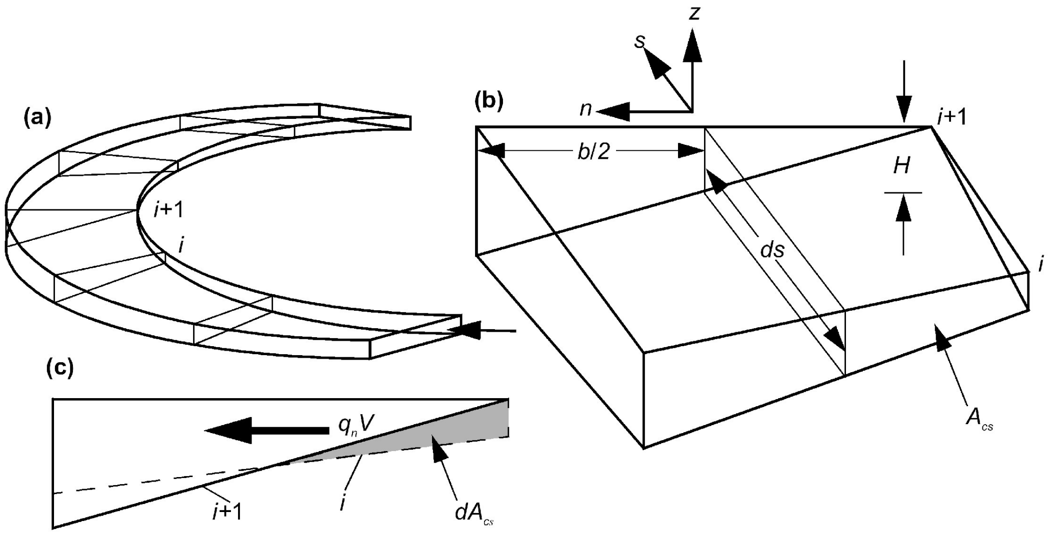

Figure 5. The channel in the CHILD model is conceptualized as a series of cross-section, e.g. i, i+1 in (a). Each cross-section (b) has an average depth H and is devided into two half-sections of width b/2, and successive sections i, i+1 are separated by an incremental downstream distance ds. The cross-sectional area for the inner half-channel (where N<0) is Acs. A lateral momentum transfer qnV results from the downstream rate of change of the inner-half cross-sectional area dAcs/ds (c).

The magnitude of a lateral force increment dF_n depends on the lateral transfer of momentum q_nV (Figure 5) from the inner half to the outer half of a channel segment ds and is defined as

$$dF_n = \rho q_n V ds \tag{3}$$

where is the water density and the lateral unit discharge q_n is given by the product of downstream flow velocity U and the change in inner-half cross-sectional area A_{cs}

$$q_n = -U \frac{dA_{cs}}{ds} \tag{4}$$

The depth-averaged lateral velocity V in equation (3) is given by

$$V = -\frac{U}{H}\frac{dA_{cs}}{ds} \tag{5}$$

Rewriting the equation (3) by substituting equations (4) and (5) holds the following expression for the lateral force increment, dF_n

$$dF_n = \frac{\rho U^2}{H}\left(\frac{dA_{cs}}{ds}\right)^2 ds \qquad (6)$$

The planform meander geometry and evolution is controlled by two important length scales, and L, present in equation (2) (Lancaster, 1998; Lancaster & Bras, 2002). The first length scale, , represents the development of a rough turbulent flow boundary layer which will tend to dissipate and decrease a velocity gradient at a the outer bank and therefore the bank shear stress. Conceptually this dissipation length scale is related to bank roughness elements such as fallen trees or boulders, where higher values for reflect smoother banks and tend to result in multibend loop formation (Lancaster and Bras, 2002). At moment no relation is established between the dimensions of these elements, and is assumed to be at the order scale of a channel width. The second length scale is the downstream lag ‘L’ and is calculated as the downstream distance travelled by water moving from one side of the channel to the opposite bank at lateral (U) and downstream velocities (V).

$$L = \frac{UB}{V} \qquad (7)$$

where B is

$$B = \frac{b}{2} + \frac{2A_{cs}}{H + h_i} \qquad (8)$$

where b the segment width, h_i is the depth at the inner bank. The bed topography used in equations (6) and (8) is approximated by a modified form of Ikeda’s (1989) equation for transverse slope

$$S_{transverse} = KHC \qquad (9)$$

$$K = \frac{\psi'}{\psi}\sqrt{\frac{\psi}{\psi_{cr}}}\left[\frac{0.2278}{\kappa}\ln\left(\frac{11.0\psi' H}{\psi d_{50}}\right) - 0.3606\right] \qquad (10)$$